



**HAL**  
open science

## Molecular mobility of poplar cell wall polymers studied by dielectric techniques

Golnaz Jafarpour Moghaddam, Eric Dantras, Alain-Michel Boudet, Colette Lacabanne

► **To cite this version:**

Golnaz Jafarpour Moghaddam, Eric Dantras, Alain-Michel Boudet, Colette Lacabanne. Molecular mobility of poplar cell wall polymers studied by dielectric techniques. *Journal of Non-Crystalline Solids*, 2008, 354 (27), pp.3207-3214. 10.1016/j.jnoncrysol.2008.01.008 . hal-03590691

**HAL Id: hal-03590691**

**<https://hal.science/hal-03590691>**

Submitted on 28 Feb 2022

**HAL** is a multi-disciplinary open access archive for the deposit and dissemination of scientific research documents, whether they are published or not. The documents may come from teaching and research institutions in France or abroad, or from public or private research centers.

L'archive ouverte pluridisciplinaire **HAL**, est destinée au dépôt et à la diffusion de documents scientifiques de niveau recherche, publiés ou non, émanant des établissements d'enseignement et de recherche français ou étrangers, des laboratoires publics ou privés.



## Open Archive Toulouse Archive Ouverte (OATAO)

OATAO is an open access repository that collects the work of Toulouse researchers and makes it freely available over the web where possible.

This is an author-deposited version published in: <http://oatao.univ-toulouse.fr/>  
Eprints ID : 2358

**To link to this article :**

URL : <http://dx.doi.org/10.1016/j.jnoncrysol.2008.01.008>

**To cite this version :** Jafarpour, G. and Dantras, Eric and Boudet, A. and Lacabanne, Colette ( 2008) *[Molecular mobility of poplar cell wall polymers studied by dielectric techniques.](#)* Journal of Non-Crystalline Solids, vol. 354 (n° 27). pp. 3207-3214. ISSN 0022-3093

Any correspondence concerning this service should be sent to the repository administrator: [staff-oatao@inp-toulouse.fr](mailto:staff-oatao@inp-toulouse.fr)

# Molecular mobility of poplar cell wall polymers studied by dielectric techniques

G. Jafarpour<sup>a</sup>, E. Dantras<sup>a,\*</sup>, A. Boudet<sup>b</sup>, C. Lacabanne<sup>a</sup>

<sup>a</sup>Laboratoire de Physique des Polymères, Institut Carnot CIRIMAT, UMR CNRS 5085, Université Paul Sabatier, Toulouse, France

<sup>b</sup>Signaux cellulaires et signalisation chez les végétaux, UMR 5546, Pôle de biotechnologies végétales, Castanet-Tolosan, France

## Abstract

In this work, thermally stimulated currents (TSC) analyzes combined with dynamic dielectric spectroscopy (DDS) have been applied to the investigation of polymers' molecular mobility involves in poplar cell wall. The molecular origin of the various dielectric relaxations has been determined. Cellulose and lignin effects in wood dielectric response were distinguished. The correlation between results obtained by both dielectric methods allows us to follow molecular mobility involved in delocalized movement as primary relaxation mode. For these two major components of wood, the evolution of relaxation times involve in  $\alpha$ -relaxation mode is explained using the strong/fragile pattern. We compared the cellulose and lignin *in situ* and *ex situ* responses to interpret wood compound behavior. The importance of structural wood interactions which modified the molecular mobility of polymer components will be underlined.

PACS: 77.22.Gm; 77.84.Jd

Keywords: Biopolymers; Dielectric properties, relaxation, electric modulus; Thermally stimulated and depolarization current; Polymers and organics

## 1. Introduction

The utilization of wood was started at prehistoric period and it is always considered as a very common raw material. Its special properties like high mechanical strength and good thermal isolation indeed its esthetic look make of wood a very modern building material. Being a renewable source of energy and the basic substance for paper and pulp, fibers, films, additives and many other products is the reason that explains the increase of world's consumption of wood. Wood is one of the most important products of nature. Its immoderate utilization causes serious ecologic and economic problems. The environmental protection, lack of energy supplies and importance of natural energy source are some reasons for

which many researchers have recently paid attentions to wood. A knowledge on physicochemical properties of wood for a better consumption seems essential now more than ever. Many researches and analyzes are performed on this natural material. By dint of studies the ultra-structure of wood composite and some of its physical and chemical properties for different species are determined. The wood tissue is in fact the walls of the vegetal cells. It is basically made of three polymers: cellulose, hemicellulose and lignin. The amount of each polymer component of wood differs drastically according to species. Some quantitative data on the chemical composition were previously given [1]. Besides the chemical properties the physical ones like mechanical and thermal response of wood were also investigated [2]. However, there are few studies on molecular mobility of wood and its constituents. Montès et al. [3] and Kelley et al. [4] were applied mechanical measurements to study relaxation behavior of the amorphous components of wood. In this work we

\* Corresponding author.

E-mail address: dantras@cict.fr (E. Dantras).

define the structure/properties relationships via molecular approach and by applying the dielectric methods. We study the dielectric properties of poplar wood and its extracted components and determine each element influence on assembly response. Static (thermally stimulated current) and dynamical (dynamic dielectric spectroscopy) dielectric techniques are used.

## 2. Experimental

### 2.1. Materials

Two years old poplar trees, grown up in a field were used for sampling. The water content of samples was  $(7.7 \pm 0.5)\%$  w/w (loss weight after 40 days over  $P_2O_5$ ). Lignin was extracted from the poplar wood samples by following chemical process: the wood chips (100 g) were introduced in an agitation reactor and impregnated by 1.5 l of acetic acid/formic acid/water (50/30/20) mix for 1 h. They were heated ( $107^\circ\text{C}$ ) for 3 h in a bain-marie. After cooling, by using Buchner filter the viscous liquid was separated. Two hundred and fifty milliliters of water was added to precipitate lignin that was subsequently collected by filtration, then washed with water and dried at room temperature. The lignin powder contained  $(4.4 \pm 0.1)\%$  w/w water. Lignin and wood samples were ground by a Danguomeau ball mill. High purity commercial cellulose powder extracted from cotton linters was provided by Sigma-Aldrich Company. Its water content was  $(4.5 \pm 0.2)\%$  w/w. All the samples were in powder shape and stored at  $4^\circ\text{C}$ . For thermally stimulated currents measurements, the powders were compacted into thin pellets (4 mm diameter and 1 mm thick). For dynamic dielectric spectroscopy measurements powders were put into a home-made capacitor with parallel discs of 10 mm in diameter, and compacted into 100–300  $\mu\text{m}$  sheets. Some sample were dried for 24 h under vacuum at  $120^\circ\text{C}$  just before measurements and called ‘dehydrated’ during this work.

### 2.2. Methods

#### 2.2.1. Thermally stimulated currents (TSC)

TSC measurements were carried out with home-made equipment developed in our laboratory, described in previous papers [5,6]. The principal of this technique is briefly reminded: a sample is inserted between two electrodes in a hermetic cell filled with dry helium. Thereafter it is polarized with a DC field  $E_p$  during a given time  $t_p$  at the temperature  $T_p$ . The sample, under the electric field, is then quenched till  $T_0 \ll T_p$  assisted by liquid nitrogen: the dipoles orientation previously induced freezes. Finally, the sample is short-circuited for a given time ( $t_{cc}$ ) to evacuate surface charges and the depolarization current due to the return to equilibrium of dipolar units is recorded. The following parameters were applied in this study:  $t_p = 2$  min,  $t_{cc} = 2$  min and  $q = 7^\circ\text{C}/\text{min}$ . The tempera-

tures  $T_p$ ,  $T_0$  and  $T_f$  were chosen according to the range of temperature in which the relaxation processes appeared. The depolarization current was registered and normalized for surface and thickness difference of the samples by using the following relation:

$$\sigma = \frac{I}{E \cdot S}, \quad (1)$$

where  $\sigma$  is the conductivity ( $\Omega^{-1} \text{m}^{-1}$ ),  $I$  the depolarization current ( $A$ ),  $E$  the applied field ( $\text{V}/\text{m}$ ) and  $S$  the polarized surface of the sample ( $\text{m}^2$ ).

In order to analyze relaxation processes, the experimental technique of fractional polarization was used. The polarization was carried out within a temperature window of  $5^\circ\text{C}$ . After short-circuiting, the cooling process was continued to a much lower temperature and the depolarization current was measured as previously described. The temperature window was then shifted by step of  $5^\circ\text{C}$ , consequently a series of elementary spectra was obtained. Each elementary spectrum is considered as a Debye peak and thus is associated with a single relaxation time  $\tau(T)$ . The temperature dependence of relaxation time can be determined by following equation:

$$\tau(T) = \frac{1}{qI(T)} \int_T^{T_f} I(T) dT, \quad (2)$$

where  $I(T)$  is depolarization current,  $q$  the heating rate and  $T_f$  the final temperature. The relaxation time  $\tau(T)$  of all the elementary spectra versus  $1/T$  is linear, and obeys to the Arrhenius–Eyring law defined as following:

$$\tau(T) = \frac{h}{k_B T} \exp \left[ -\frac{\Delta S}{R} \right] \exp \left[ \frac{\Delta H}{RT} \right] = \tau_{0a} \exp \left[ \frac{\Delta H}{RT} \right], \quad (3)$$

where  $k_B$  is the Boltzmann constant,  $R$  the gas constant,  $h$  Planck constant,  $\tau_{0a}$  the pre-exponential factor,  $\Delta H$  the activation enthalpy and  $\Delta S$  the activation entropy. The following relation, called the compensation equation, described the temperature dependence of the relaxation time ( $\tau$ )

$$\tau(T) = \tau_C \exp \left[ \frac{\Delta H}{R} \left( \frac{1}{T} - \frac{1}{T_C} \right) \right], \quad (4)$$

where  $T_C$  and  $\tau_C$  are the compensation temperature and the compensation time, respectively. The compensation law explained that all the relaxing entities with different length have the same relaxation time ( $\tau_C$ ) at the compensation temperature ( $T_C$ ) [7].

As for most polymers, the primary mode could be described by a Vogel–Tamman–Fulcher (VTF) equation. Vogel–Tammann–Fulcher equation can formulate the relaxation time evolution versus the inverse of temperature:

$$\tau(T) = \tau_{0v} \exp \left[ \frac{B}{T - T_0} \right], \quad (5)$$

where  $\tau_{0v}$  is the pre-exponential factor,  $B$  and  $T_0$  are the constants.

### 2.2.2. Dynamic dielectric spectroscopy (DDS)

A novocontrol broadband dielectric spectrometer system BDS 400 was used to obtain the dielectric relaxation maps in extended temperature and frequency scales. Isothermal measurements were carried out in the frequency range of  $10^{-1}$ – $10^6$  Hz for temperature varying from  $-150$  to  $200$  °C by steps of  $5$  °C. The complex dielectric constant  $\epsilon^*(\omega)$  was recorded. This relaxation process was evaluated by Havriliak–Negami function [9,10]:

$$\epsilon^*(\omega) = \epsilon_\infty + \frac{\Delta\epsilon}{[1 + (i\omega\tau_{\text{HN}})^{\alpha_{\text{HN}}}]^{\beta_{\text{HN}}}}, \quad (6)$$

where  $\tau_{\text{HN}}$  is the relaxation time of Havriliak–Negami (HN) model and  $\alpha_{\text{HN}}$  and  $\beta_{\text{HN}}$  characterize respectively the width and the asymmetry of the relaxation time distribution. In order to resolve the overlapping peaks in dielectric loss responses (e.g.  $\alpha$ -relaxation and Maxwell–Wagner–Sillars or electrode depolarization), a convenient technique was proposed by the team of Van Turnhout [11]. This analytic method is based on the approximation of the logarithmic derivative of the real dielectric permittivity by the dielectric loss:

$$\epsilon''_{\text{deriv}} \approx \frac{\pi\partial\epsilon'(\omega)}{2\partial\ln\omega} = \epsilon''. \quad (7)$$

For broad relaxations,  $\epsilon''_{\text{deriv}}$  is a fair approximation of the Kramers–Kronig transformation. This method which has been successfully applied in the literature, is very useful to separate superimposed relaxation modes [12,13].

## 3. Results

### 3.1. Lignin

#### 3.1.1. Thermally stimulated currents

Dielectric behavior of lignin was studied by thermally stimulated currents method. A secondary relaxation process was observed between  $-120$  and  $-50$  °C. It was centered at  $-86$  °C and named  $\beta_{\text{lin}}$ -relaxation mode. This secondary mode could be assigned to localized movements of chain segments. Hydration had an anti-plasticizer effect on these movements, i.e. made the relaxing entities less mobile. A second relaxation mode, named  $\alpha_{\text{lin}}$  was recorded at higher temperature. Its maximum was situated at  $106$  °C. This primary relaxation process could be attributed to the dielectric manifestation of lignin glass transition.  $\alpha_{\text{lin}}$ -relaxation mode is shifted of  $25$  °C to higher temperature after the thermal treatment. So water molecules made easier the delocalized chain movements and in contrast to  $\beta_{\text{lin}}$ -relaxation, hydration at this stage had a plasticizer effect. The series of elementary spectra for  $\alpha_{\text{lin}}$ -relaxation mode was obtained by technique of fractional polarization (Fig. 1). The  $5$  °C polarization window was moved from  $85$  to  $135$  °C. The dehydrated sample was used to minimize the modification of complex mode before and after this experimental deconvolution (complex thermo-

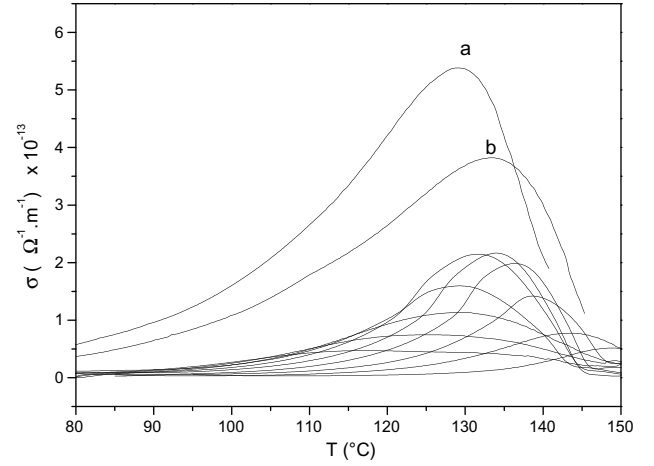


Fig. 1. Elementary thermograms of  $\alpha$ -relaxation process for lignin; ‘a’ and ‘b’ are respectively the complex modes before and after the experimental deconvolution, the polarization temperatures were respectively  $T_P = 140$  and  $145$  °C.

grams called a and b in Fig. 1). As for wood samples, the compensation diagram was obtained and shown in Fig. 2. The six first elementary spectra revealed a compensation phenomenon. The linear dependence of activation enthalpy and entropy was observed as well. The compensation parameters are calculated as following:  $\tau_C = 2.94$  s and  $T_C = 162$  °C. This phenomenon for  $\alpha$ -mode underlined the cooperativity of chain segmental movements.

#### 3.1.2. Dynamic dielectric spectroscopy

The complex dielectric permittivity  $\epsilon^*$  was measured for lignin samples. The temperature varied from  $-150$  to  $200$  °C by steps of  $5$  °C. Between  $-100$  and  $0$  °C, the first relaxation process was observed. It corresponded to the secondary  $\beta_{\text{lin}}$ -relaxation recorded by TSC measurements at the same temperature range. Applying the Havriliak–Negami equation, temperature dependence of relaxation time was studied and shown in Fig. 3. The linear evolution of relaxation time revealed Arrhenius behavior for this

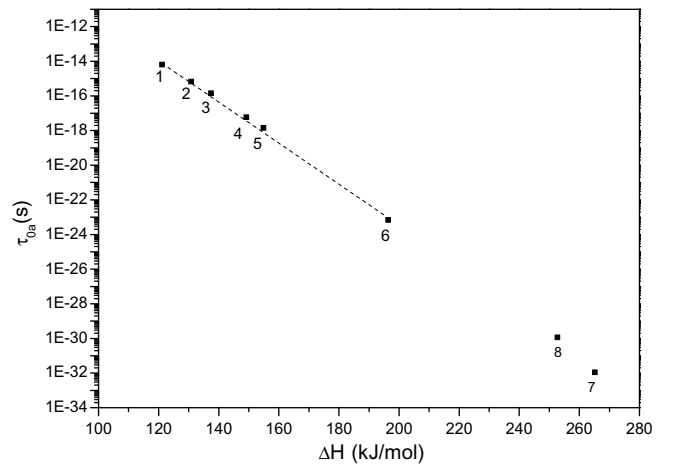


Fig. 2. Compensation diagram of  $\alpha$ -relaxation mode of lignin.

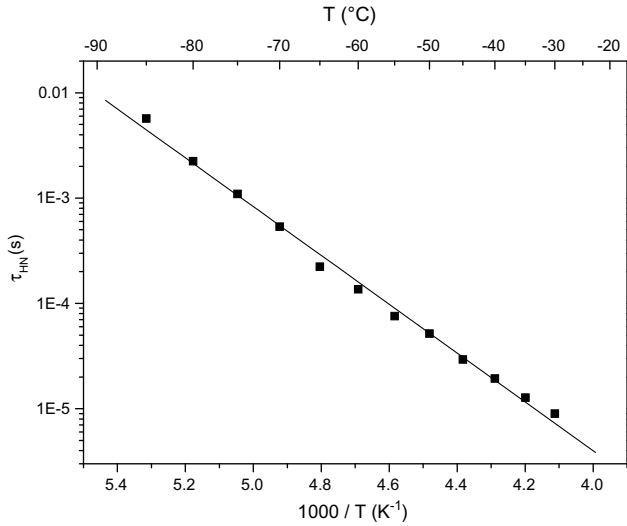


Fig. 3. Arrhenius diagram for low temperature relaxation mode of lignin obtained by DDS.

relaxation mode. Pre-exponential factor  $\tau_{0a}$  and activation enthalpy  $\Delta H$  values are the  $y$ -intercept and the slope of line, respectively. They are calculated as  $\tau_{0a} = 2.13 \times 10^{-15}$  s and  $\Delta H = 44.4$  kJ mol $^{-1}$ . The activation entropy  $\Delta S$  was also obtained and equal to 38.7 J mol $^{-1}$  K $^{-1}$ .

At higher temperature, two isothermal peaks centered at 30 and 130 °C were recorded. The first one could be compared to the isothermal signal observed for cellulose and also for wood in the same temperature range. These two peaks were associated with water presence in samples because they disappeared for dehydrated substances.

At last, at high temperature and low frequency range, appearance of electrode polarization hid the  $\alpha_{lin}$ -relaxation mode of lignin. In order to distinguish the superimposed relaxations other analyzes method should be applied, as proposed by Steeman et al. (cf. Eq. (7)). The results obtained for temperature range of 165/190 °C are presented in Fig. 4. The temperature dependence of relaxation time is not linear. In fact, in most of polymers as soon as the temperature approaches the glass transition or goes over it, the relaxation time deviates from the Arrhenius equation and shows a non-linear dependence on temperature: it is characteristic of a VTF behavior (cf. Eq. (5)). For  $\alpha_{lin}$ -relaxation mode like many other primary relaxation mode at high temperature range VTF relation could be applied. The fitting parameters are calculated as  $\tau_{0v} = 2.88 \times 10^{-9}$  s,  $B = 1915$  K and  $T_0 = 324$  K.

### 3.2. Cellulose

Dielectric behavior of cellulose was studied by TSC and DDS methods and extensively published in a previous article [14]. It is interesting to briefly remind some results: three relaxation processes were observed, two in low temperature range ( $-170 < T < 0$  °C) so called  $\gamma_{cell}$  and  $\beta_{cell}$ . They are

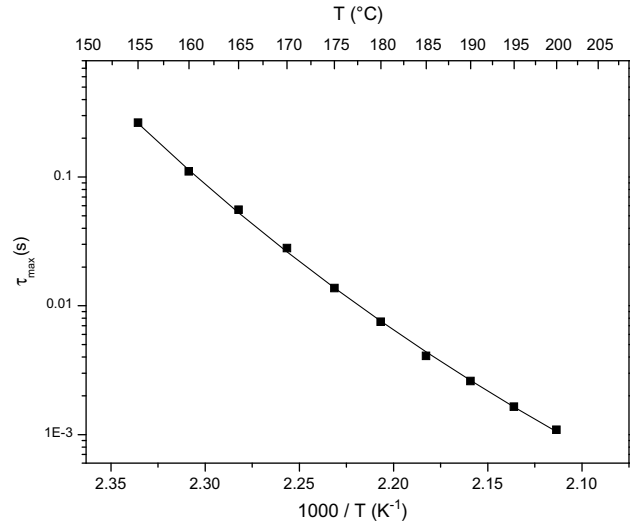


Fig. 4. Temperature dependence of relaxation time for  $\alpha$ -relaxation mode of dehydrated lignin.

respectively related to side group and segmental backbone movements. The third relaxation mode  $\alpha_{cell}$  was observed in high temperature range ( $50 < T < 200$  °C). This relaxation mode was associated with cooperative movements of cellulose chain. We concluded that it could be the dielectric manifestation of glass transition.

### 3.3. Wood

#### 3.3.1. Thermally stimulated currents

The dielectric measurements were performed by TSC to study relaxation behavior of poplar wood. The following parameters were used:  $T_p = 120$  °C,  $T_0 = -170$  °C and  $T_f = 130$  °C. As showed in Fig. 5, four dielectric relaxation processes were observed. At low temperature ( $T < 0$  °C), two relaxation modes were observed. The first one called  $\gamma$ -relaxation mode was situated between  $-160$  and

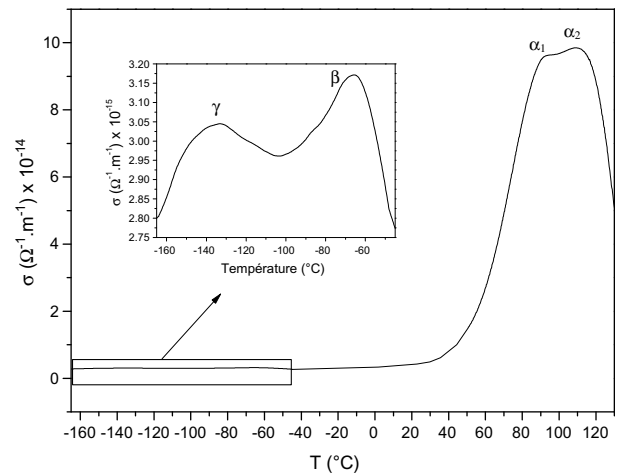


Fig. 5. Dielectric relaxation processes for poplar wood samples obtained by TSC method.

–100 °C with a maximum about –135 °C. The second one, located between –100 and –50 °C and centered at –65 °C named  $\beta$ -relaxation mode. We showed that  $\gamma$ -mode was attributed to side group movements of amorphous zone of cellulose while  $\beta$ -relaxation to its segmental backbone movements.

In the temperature range from 40 to 130 °C, two other relaxation modes  $\alpha_1$  and  $\alpha_2$  were extracted. They had the same magnitude but they merged. As shown in Fig. 5 maxima of  $\alpha_1$  and  $\alpha_2$  were respectively situated at about 95 and 108 °C. For  $\alpha_1$  and  $\alpha_2$  the polarization window of 5 °C was shifted between 70 and 110 °C. The complex and elementary spectra of wood are shown in Fig. 6.

In Fig. 7, Arrhenius temperature dependence of relaxation time for the series of elementary thermograms is illustrated. The values of  $\tau_{0a}$  and  $\Delta H$  are the  $y$ -intercept and the

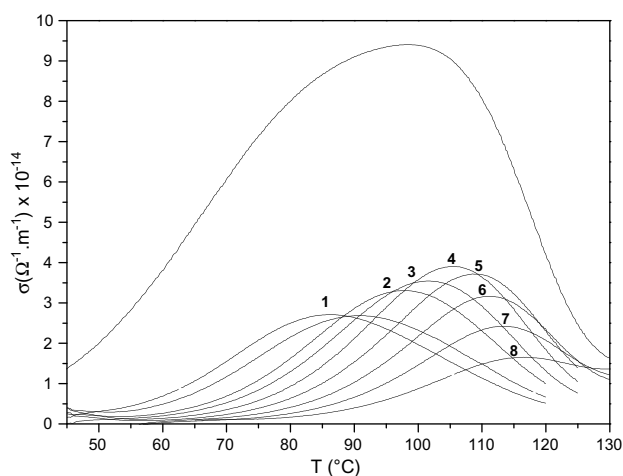


Fig. 6. Complex and elementary thermograms of poplar wood for high temperature relaxation modes  $\alpha_1$  and  $\alpha_2$ .

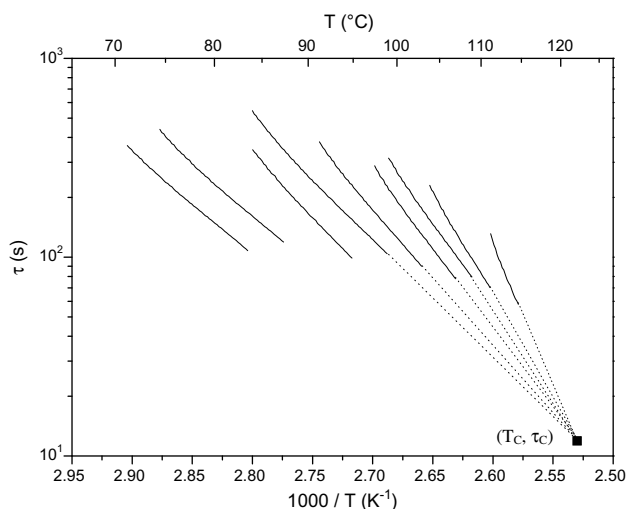


Fig. 7. Arrhenius diagram of elementary spectra related to  $\alpha_1$  and  $\alpha_2$  relaxation processes.

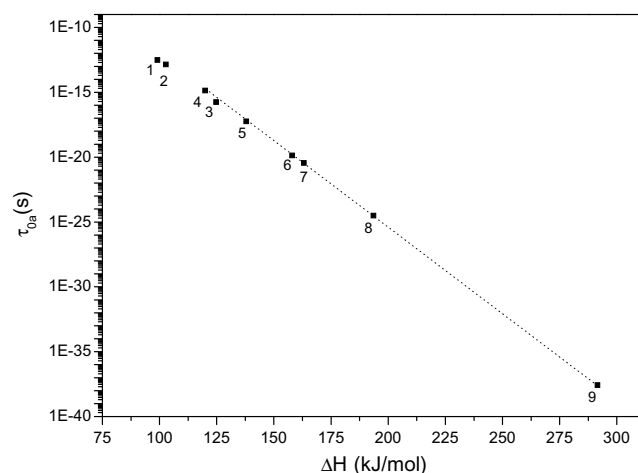


Fig. 8. Compensation diagram of high temperature relaxation modes of wood samples.

slope of lines, respectively. They are calculated for each elementary peak (each line) and shown in Fig. 8. In this diagram, named compensation diagram, the linear dependence of activation enthalpy and entropy is illustrated ( $\tau_{0a}$  and  $\Delta S$  have linear dependence cf. Eq. (3)). The compensation point ( $T_C$ ,  $\tau_C$ ) shown in Fig. 7 was calculated through this equation as following:  $T_C = 122$  °C and  $\tau_C = 11.9$  s. The six later lines related to the six elementary spectra converged to the compensation point. This phenomenon was interpreted as an effect of cooperative movements [8]. So the high temperature relaxation processes,  $\alpha_1$  and  $\alpha_2$ , are attributed to the cooperative movements of polymer chain.

### 3.3.2. Dynamic dielectric spectroscopy

The DDS isothermal measurements were performed in a frequency range from  $10^{-1}$  to  $10^6$  Hz, for temperature varying between –150 and 200 °C by steps of 5 °C. One relaxation process was observed at  $T < 0$  °C. Its maximum was situated at –113 °C for a frequency of  $10^{-1}$  Hz and at –30 °C for  $10^6$  Hz. The HN-fitting parameters for the isothermal spectrum in temperature range of relaxation process were determined. In Fig. 9 the relaxation time evolution  $\tau_{HN}$  versus  $1/T$  for the natural and dehydrated samples in the temperature range from –100 to –30 °C was shown. In the both case the temperature dependence of relaxation time followed the Arrhenius Eq. (3). By applying Eq. (3) and the line fitting values the function parameters were calculated as:  $\tau_{0a} = 1.23 \times 10^{-19}$  s,  $\Delta H = 57.5$  kJ mol $^{-1}$  and  $\Delta S = 120$  J mol $^{-1}$  K $^{-1}$  for natural sample and  $\tau_{0a} = 3.3 \times 10^{-12}$  s,  $\Delta H = 28.8$  kJ mol $^{-1}$  and  $\Delta S = 3.09$  J mol $^{-1}$  K $^{-1}$  for dehydrated one. The decrease of the activation enthalpy value shows the anti-plasticizer effect of water molecules on secondary relaxation mode of wood.

One isothermal phenomenon was registered for natural samples of poplar wood. Its maximum was situated at 39 °C for all the frequency range. The same process was

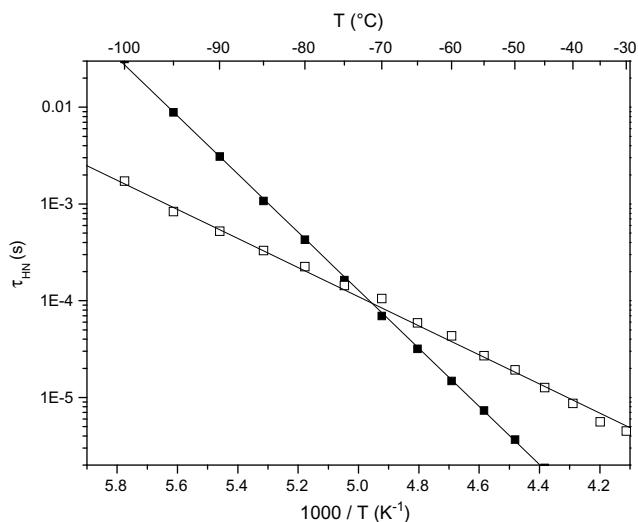


Fig. 9. Arrhenius diagram for secondary relaxation process of hydrated (■) and dehydrated (□) poplar wood samples obtained by DDS method.

observed for cellulose sample and assigned to freezing water found in the substances [14]. Same as for cellulose samples, it did not appear during second temperature scanning or after a thermal treatment at 120 °C.

At high temperature ( $T > 160$  °C) two relaxation modes were obtained numerated '1' and '2'. Evolution of dielectric loss  $\epsilon''$  versus the frequency for temperature of  $165^\circ\text{C} < T < 200$  °C is illustrated on Fig. 10. The two relaxation processes were analyzed by applying the Havriliak–Negami Eq. (6). Relaxation time evolution versus temperature is shown in Fig. 11. The two relaxation modes pointed out a linear temperature dependence of relaxation time. The activation enthalpy ( $\Delta H$ ) and the pre-exponential factor ( $\tau_{0a}$ ) values were  $143.15 \text{ kJ mol}^{-1}$  and  $4.6 \times 10^{-19} \text{ s}$  for mode '1', respectively. The activation entropy ( $\Delta S$ ) was determined equal to  $115.39 \text{ J mol}^{-1} \text{ K}^{-1}$  for this pro-

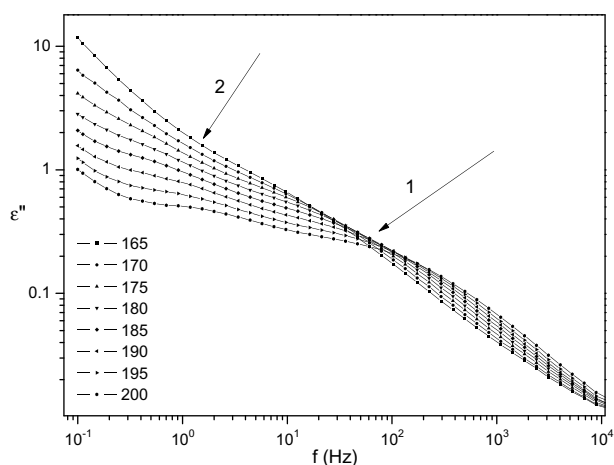


Fig. 10. Isothermal spectra of wood sample for temperature range of  $165^\circ\text{C} < T < 200$  °C obtained by DDS.

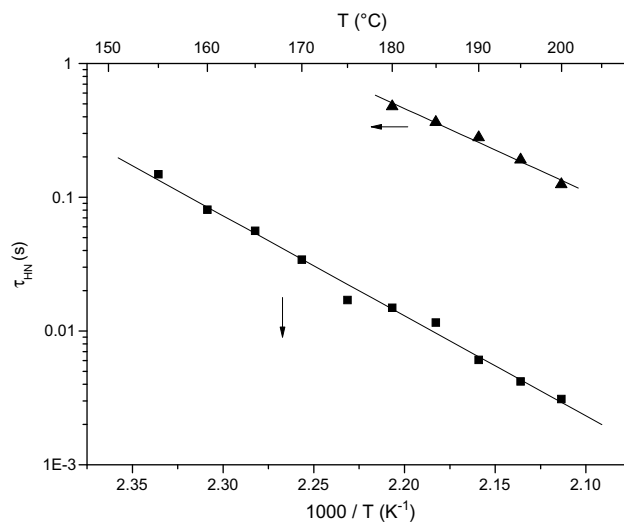


Fig. 11. Arrhenius diagram for high temperature relaxation modes, '1' (■) and '2' (▲) of poplar wood.

cess. For mode '2'  $\Delta H = 118.68 \text{ kJ mol}^{-1}$ ,  $\tau_{0a} = 1.05 \times 10^{-14} \text{ s}$  and  $\Delta S = 18.97 \text{ J mol}^{-1} \text{ K}^{-1}$  were calculated.

#### 4. Discussion

In order to better understand dynamic properties of wood, we compared the dynamic dielectric results of wood with the one of its major polymeric components i.e. cellulose and lignin. For the purpose of clarity, primary and secondary dielectric relaxation modes corresponding to higher and lower temperature ranges are discussed separately:

##### 4.1. Secondary relaxation modes at lower temperature ( $T < 0$ °C)

We investigated by TSC the temperature position of secondary relaxation modes of wood, cellulose and lignin. We observed pertinent similarities between the temperature maxima of  $\gamma_{\text{cell}}$  and  $\beta_{\text{cell}}$  (of cellulose) and  $\gamma$  and  $\beta$  of wood. On the contrary, the secondary relaxation mode of lignin was completely shifted and conformed to neither  $\gamma$  nor  $\beta$ -relaxation mode. The analogous conclusion was obtained by DDS. In Fig. 12 the evolution of relaxation time versus inverse temperature are presented for three substances: wood, cellulose and lignin. Wood and cellulose responses are superposed while lignin response was quite different. According to these observations we concluded that the localized relaxation movements in wood at low temperature are related to those of cellulosic component. So these mobilities are essentially related to the molecular mobility of ( $-\text{OH}$ ) and ( $-\text{CH}_2\text{OH}$ ) side groups of cellulose. The wood interactions made difficult lignin localized movements. Lignin forms a more complicated network with its environment in wood structure and its movements are

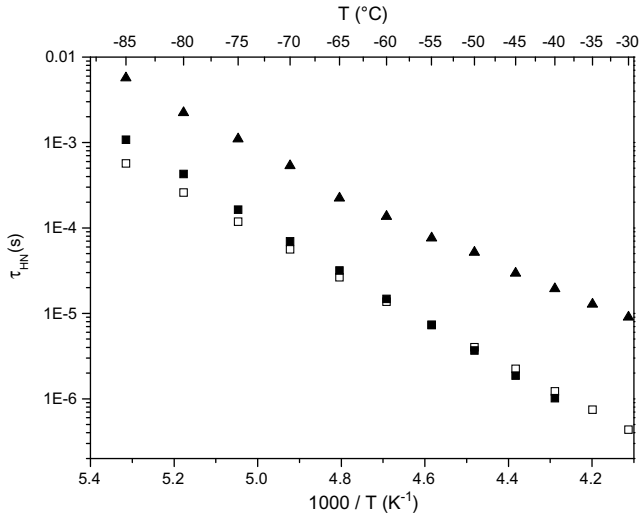


Fig. 12. Comparison of low temperature dielectric responses of poplar wood (■), cellulose (□) and lignin (▲).

strongly decreased while cellulose is less involved in interactions.

#### 4.2. Primary relaxation modes at higher temperature ( $T > 0^\circ\text{C}$ )

The results obtained by TSC and DDS for wood, cellulose and lignin are presented in the same graph for the purpose of comparison. Temperature dependence of relaxation times for all polymeric substances are reported on Fig. 13. TSC corresponds to the lower frequency range data, DDS to the higher frequency range data. The DDS results, situated at higher frequency (lower relaxation time) are extrapolated towards lower frequency reaching the range of TSC data.

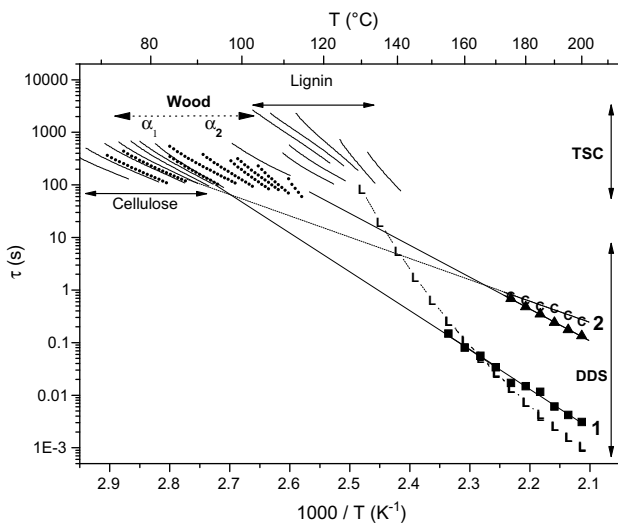


Fig. 13. Correlation between DDS and TSC results in the high temperature range; 1 (■) and 2 (▲) are two dielectric relaxation modes of poplar wood, («C»)  $\alpha_{\text{cell}}$ -process of cellulose and («L»)  $\alpha_{\text{lin}}$ -process of lignin observed by DDS. In the low temperature range, relaxation modes in wood samples (*in situ*) in bold lines, extracted lignin and cellulose (*ex situ*) are in normal lines.

For cellulose, the extrapolation of DDS linear dependence (symbolised by ‘C’ on the diagram) corresponds to the linear TSC data. Such an Arrhenius behavior for the  $\alpha$ -relaxation time from glassy to liquid state, has been already described as the ‘strong’ behavior [14]. It is coherent with the absence of heat capacity step on differential scanning calorimetry thermograms [15–19]. The high density of hydrogen bonds in cellulose explains such a strong behavior.

For lignin, the VTF dependence (symbolised by ‘L’ on the diagram) intercepts the TSC linear dependence at the maximum temperature of the TSC peak. This discontinuity in the temperature dependence of the  $\alpha$ -relaxation time is characteristic of a ‘fragile’ behavior. Note that this behavior is accompanied by a significant step on the DSC thermogram. The low density of hydrogen bonds in lignin is coherent with the observation of a fragile behavior.

For wood, the correlation between the two dielectric responses allows us to specify the molecular origin of relaxation modes. First of all, the origin of the sub modes number ‘1’ and ‘2’ obtained by DDS must be clarified. The sub mode ‘1’ appeared in the near vicinity of the one of lignin, besides the sub mode ‘2’ is close to the one of cellulose. Consequently, the sub mode ‘1’ has been attributed to segmental movements of lignin and sub mode ‘2’ to segmental movements of cellulose.

The comparison between DDS and TSC results has been used to clarify the molecular origin on the sub modes in the vitreous state. Extrapolation of the sub mode ‘1’, related to lignin corresponds to the  $\alpha_1$  sub mode on the lower temperature side. Extrapolation of sub mode ‘2’, assigned to relaxing entities of cellulose, corresponded to the  $\alpha_2$  sub mode, on the higher temperature side. So  $\alpha_1$  and  $\alpha_2$  were respectively attributed to lignin and cellulose segmental movements.

Owing to the combination of DDS/TSC data, we are able to follow the role of interactions between the various polymeric components of wood, by making a comparison of *in situ* and *ex situ* analysis. The line slope increased for cellulose in wood matrix (▲) in comparison with pure cellulose (‘C’). This revealed the increase of activation enthalpy ( $\Delta H$ ) for this relaxation mode (‘1’). In fact cellulose chain movements decreased *in situ* which was provoked by the strong interaction of wood. The important influence of wood interaction was confirmed by analyzing lignin behavior. For lignin the VTF temperature dependence of relaxation time for its primary relaxation ( $\alpha_{\text{lin}}$ ) modifies to Arrhenius behavior in wood complex (respectively ‘L’ and (■) on figure).

For the natural composite, we do not pointed out a discontinuity in the behavior law of relaxation times from glassy to liquid state. Wood is considered as a ‘strong’ composite.

## 5. Conclusion

In this work we investigated and analyzed the dielectric properties of wood by DDS and TSC methods. We compared wood responses with its two major constituents

(cellulose and lignin) to determine the origin of the dielectric relaxations and interpret wood compound behavior. Cellulose and lignin effects in wood dielectric responses of TSC and DDS were distinguished. We assigned low temperature relaxation of wood to cellulose chain segmental movements. In the high temperature range we defined the origin of each dielectric relaxation mode of wood regarding to its components. We also showed the importance of structural wood interactions which modified the components behavior *in situ*. It is interesting to note that low frequency range of dielectric techniques shed some light on physical structure and hydrogen bonding more particularly. The influence of chemical structure is underlined in the high frequency range.

### Acknowledgment

The authors thanks 'Unité Amélioration, Génétique et Physiologie Forestières' of INRA in Orléans for providing lignin.

### References

- [1] D. Fengel, G. Wegener, Wood: Chemistry, Ultrastructure, Reactions, in: W. de Gruyter (Ed.), Berlin, New York, 1984.
- [2] Forest Products Laboratory, Wood handbook: Wood as an Engineering Material, Madison, WI, USDA, 1999.
- [3] H. Montès, K. Mazeau, J.Y. Cavaillé, *Macromolecules* 30 (1997) 6977.
- [4] S.S. Kelley, T.G. Rials, W.G. Glasser, *J. Mater. Sci.* 22 (1987) 617.
- [5] G. Teyssède, C. Lacabanne, *J. Phys. D: Appl. Phys.* 28 (1995) 1478.
- [6] G. Teyssède, S. Mezghani, A. Bernès, C. Lacabanne, in: J. P. Runt, J.J. Fitzgerald (Ed.), *Dielectric Spectroscopy of Polymeric Materials-Fundamental and Application*, 1997.
- [7] J.D. Hoffman, G. Williams, E. Passaglia, *J. Polym. Sci.* 14 (1966) 173.
- [8] C. Lacabanne, A. Lamure, G. teyssède, A. Bernès, M. Mourgues, *J. Non-Cryst. Solids* 172-174 (1994) 884.
- [9] S. Havriliak Jr., S. Negami, *J. Polym. Sci. C* 14 (1966) 99.
- [10] S. Havriliak Jr., S. Negami, *Polymer* 8 (1967) 161.
- [11] P.A.M. Steeman, J. van Turnhout, *Macromolecules* 27 (1994) 5421.
- [12] M. Wübbenhorst, J.V. Turnhout, *J. Non-Cryst. Solids* 305 (2002) 40.
- [13] A. Molak, M. Paluch, S. Pawlus, J. klimontko, Z. Ujama, I. Gruszka, *J. Phys. D: Appl. Phys.* 38 (2005) 1450.
- [14] G. Jafarpour, E. Dantras, A. Boudet, C. Lacabanne, *J. Non-Cryst. Solids* 353 (2007) 4108.
- [15] L. Stubberud, H.G. Arwidsson, A. Larsson, C. Graffner, *Int. J. Pharm.* 134 (1996) 79.
- [16] E. Maltini, D. Torreggiani, E. Venir, G. Bertolo, *Food Chem.* 82 (2003) 79.
- [17] M. J. Gidley, D. Cooke, S. Ward-smith, Low-moisture polysaccharide systems: thermal and spectroscopy aspects, in: J. M. V. Blanshard, P. J. Lillford (Ed.), *The Glassy State in Foods*, Nottingham, 1993.
- [18] Y.H. Roos (Ed.), *Phase Transition in Foods*, Academic Press, San Diego, 1995.
- [19] S. Hadano, K. Onimura, H. Tsutsumi, H. Yamasaki, T. Oishi, *J. Appl. Polym. Sci.* 90 (2003) 2059.